Determining Optimal Setting for AMIENext Procedure Using Iridium Data

Yining Shi[1], Tomoko Matsuo[1], Delores Knipp[1], Liam Kilcommons[1], Brian Anderson[2]
[1]CU Aerospace Engineering Sciences (ASEN), [2]JH Applied Physics Laboratory (APL)

Abstract

The Assimilative Mapping of Ionospheric Electrodynamics Next (AMIENext) procedure developed by Matsuo et al. (2015) generates magnetic potential and field-aligned current (FAC) patterns in the high-latitude region by assimilating Iridium magnetic perturbation data provided by the AMPERE program using the optimal interpolation (OI) method. As expected, AMIENext results vary with the choice of assimilation procedure settings including

- **Use of sample mean vs. empirical model as background**
- **Use of different windows for estimation of mean and Empirical Orthogonal Functions (EOFs)**
- **Number of EOFs used to parameterize the background covariance**

We evaluate the performance of AMIENext and determine an optimal setting using cross validation analysis against AMPERE and DMSP magnetic perturbation data. Results show the use of sample mean estimated from Iridium data as the background instead of the empirical model developed by Weimer (2005) and the use of shorter windows leads to a better agreement with validation data set. Using more EOFs generally improves the model-data agreement, but produces higher outliers.

Data – Iridium Magnetic Perturbation

Iridium constellation is a commercial communication satellite constellation that provides global coverage at an altitude around 780 km. Engineering grade magnetometers onboard the satellites measure the magnetic field strength in along and across-track directions. **A**ctive **M**agnetosphere and **P**lanetary **E**lectrodynamics **R**esponse **E**xperiment (AMPERE) program provides Iridium perturbation data pre-processed for scientific research with a 20-sec cadence in normal operation, 2-sec in high resolution mode.

Only cross-track data are extracted in our project because of a higher uncertainty of along-track data due to attitude control in aging spacecraft. Figure 1 shows the data coverage for a 36-min interval with 20-sec cadence at 11:40 UT on May 29th, 2010.

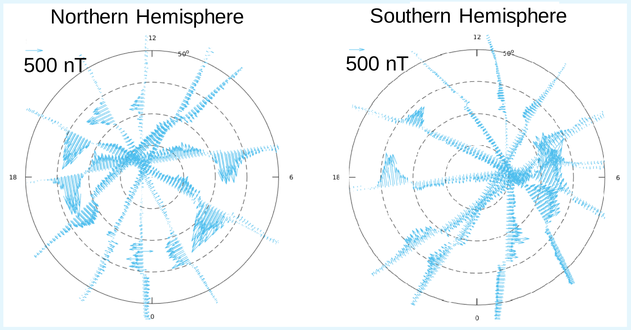

Figure 1: 36-min interval cross-track AMPERE data

Empirical Orthogonal Function (EOF) and Sample Mean Analysis

AMPERE data are first decomposed using the method described in Matsuo et al., 2002 into the EOFs that characterize the dominant modes of variability in the data as follows

$$\boldsymbol{\delta B}'(\mathbf{r},t) = \boldsymbol{\delta B}(\mathbf{r},t) - \overline{\boldsymbol{\delta B}}(\mathbf{r},t)$$

$$\boldsymbol{\delta B}'(\mathbf{r},t) = \alpha^{(1)}(t)\cdot \mathbf{EOF}^{(1)}(\mathbf{r}) + \alpha^{(2)}(t)\cdot \mathbf{EOF}^{(2)}(\mathbf{r}) + \cdots + \mathbf{e}'(\mathbf{r},t)$$

where $\overline{\boldsymbol{\delta B}}(\mathbf{r},t)$ is the sample mean of data set $\boldsymbol{\delta B}(\mathbf{r},t)$; $\alpha^{(i)}(t)$ are the time-dependent coefficients for $\mathbf{EOF}^{(i)}(\mathbf{r})$.

- The mean and EOFs are expressed in terms of a set of 244 modified polar-cap spherical harmonic basis functions (Richmond and Kamide, 1988).
- The mean magnetic perturbation is estimated from a weighted linear regression of the data on the basis functions. The inverse of the data uncertainty calculated following the method described in Cousins et al. (2015) is used as the weight in the regression.

Figure 2 shows contours of the northern hemisphere magnetic potential mean and first three EOFs estimated from data in the 36-min window. Iridium tracks are plotted on the mean pattern.

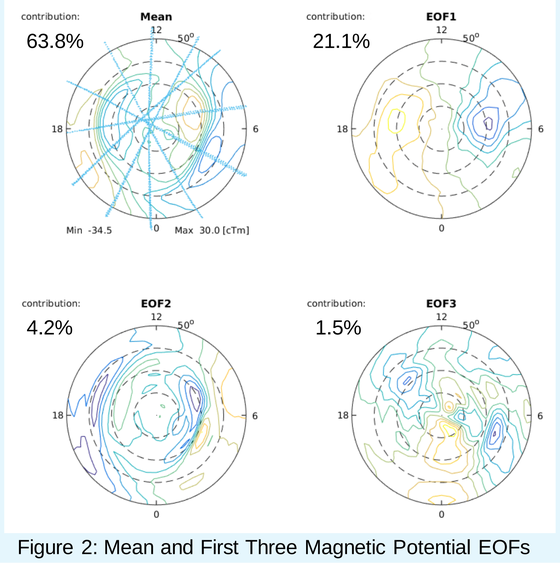

Figure 2: Mean and First Three Magnetic Potential EOFs

Impacts of the Background Model and Background Error Covariance on AMIENext Analyses

Optimal interpolation (OI) analyses of magnetic potential and FAC are generated from the new AMIENext procedure (Matsuo, 2015) by assimilating observations over 4 minutes every 2 minutes for May 29th, 2010. AMIENext results depend on the choice of background model, background error covariance, observational error covariance and other parameters. Figure 3 shows AMIENext magnetic potential pattern in line contours and FAC pattern in color contours for both hemispheres at 11:40 UT on May 29th, 2010 using different time windows to construct the mean and EOFs: 36-min (top) and one day (bottom). The same 4-minute window data are used for the OI analysis. The shorter window produces more intense FACs. Therefore, it is important to determine an optimal setting for AMIENext procedure.

Dst = -67 nT
At 11:40 UT

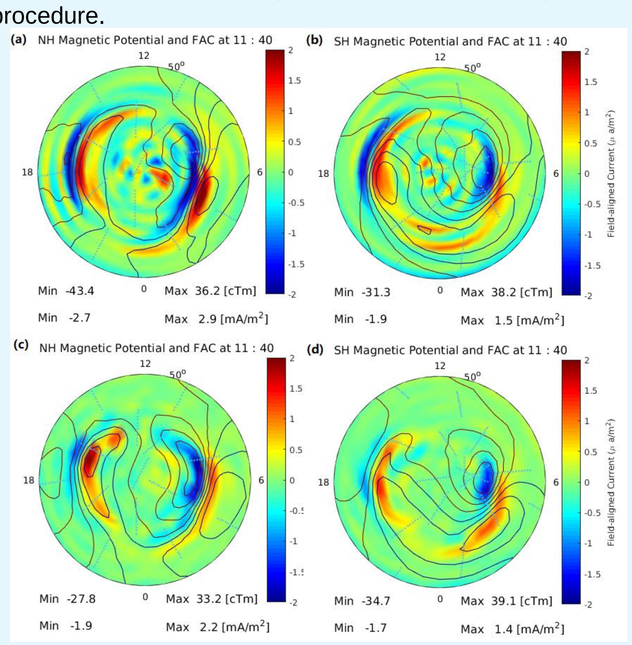

Mean and EOF window = 36 min

Mean and EOF window = one day

Figure 3: AMIE magnetic potential and FAC patterns with different EOF windows

Background Model and Error Covariance

Combinations of background models and background covariance matrices listed in Table 1 are tested using cross validation in this presentation.

	Background Model	Background Covariance
20min	+/- 10-min data mean	+/ 10-min data 3 EOFs
36min	+/- 18-min data mean	+/- 18-min data 3 EOFs
1day	One day data mean	One day data 3 EOFs
1day5EOF	One day data mean	One day data 5 EOFs
1week7EOF	One week data mean	One week data 7 EOFs
Weimer	Weimer model	+/- 18-min data 3 EOFs

Table 1: Background Model and Background Covariance Combinations

Cross Validation

To compare the performance of different parameter settings, we use

- 10-fold cross validation against Iridium data that are excluded from the estimation process as independent validation set, and
- comparison to Defense Meteorological Satellite Program(DMSP) F16, F17 and F18 data along DMSP satellite tracks.

To evaluate the difference between estimations and observations quantitatively, we calculate the following statistics

- root-mean-square vector error (RMSE) $|\mathbf{dB}_{\text{estimation}} - \mathbf{dB}_{\text{observation}}|$,
- median absolute error $|\mathbf{dB}_{\text{estimation}}| - |\mathbf{dB}_{\text{observation}}|$
- ratio $\mathbf{dB}_{\text{estimation}}/\mathbf{dB}_{\text{observation}}$.

Results

Figure 4 summarizes the cross validation results against Iridium data using three different statistical measures in boxplots for both hemispheres. Median and interquartile values are shown with the red lines and blue boxes. The maximum whisker length is 1 times the interquartile range. Outliers for 20min case and Weimer case are clipped for the purpose of showing other features.

- Comparing to the Weimer model, the use of sample mean as the background results in a better agreement. Weimer case results in positive biases while sample mean cases results in slightly negative biases.
- The mean and covariance estimated using shorter windows (20min and 36min) result in a better agreement than the case using either a day or a week window. The use of 20-min windows results in some very high outliers and underperforms comparing to the case using 36-min windows here.
- The use of 5 EOFs (rather than 3) to construct the background error covariance improves the median and interquartile ranges slightly, but results in some higher outliers. Further studies with larger data sets are required for other window lengths to better understand the influence of using different numbers of EOFs to construct the covariance matrix.

Table 2 shows the mean and median vector RMSE between AMIENext estimations and DMSP observations for both hemispheres using 36-min windows. These values are comparable to the discrepancy found between AMPERE and DMSP observations during the same time period discussed in Knipp et al. (2014).

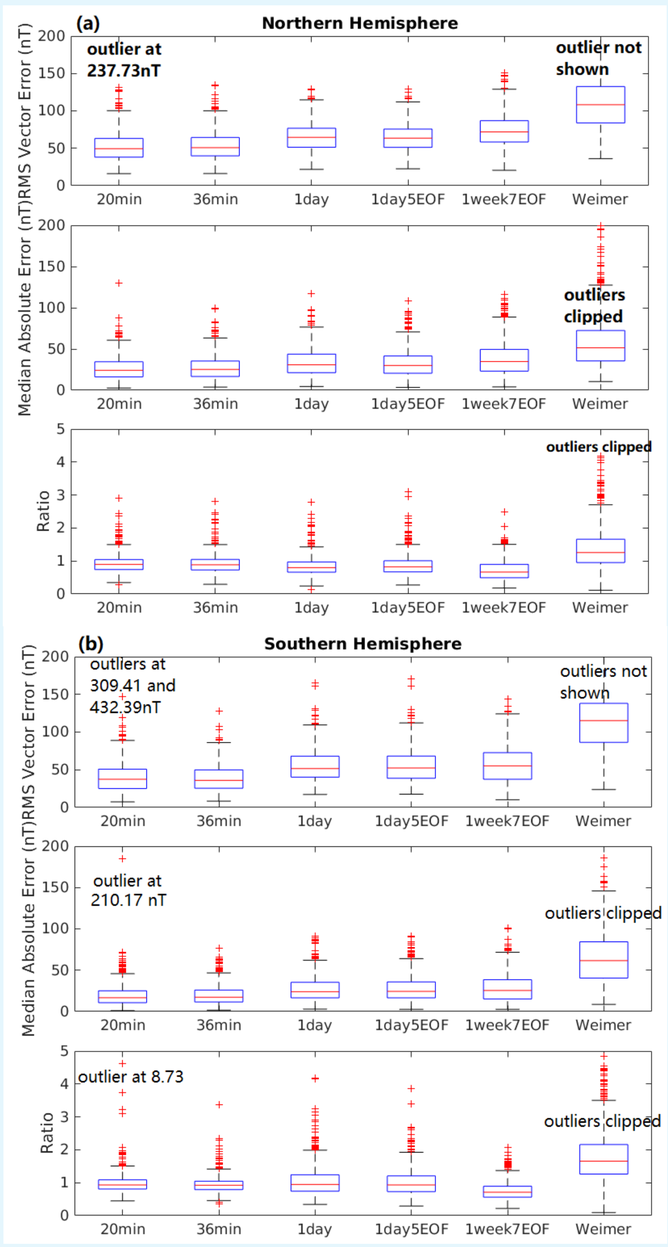

Figure 4: Cross Validation Results for Northern (a) and Southern (b) hemisphere

	Mean RMSE (nT)	Median RMSE (nT)
Northern Hemisphere	147.65	97.02
Southern Hemisphere	128.21	76.70

Table 2: Vector RMSE between AMIENext estimations and DMSP observations

Conclusions

We used cross validation to determine the optimal settings for AMIENext procedure.

We found estimations to be closer to Iridium observations when using

- **a sample mean instead of the empirical model as the background**
- **a shorter window to construct the sample mean and EOFs**
- **more EOFs to construct the background covariance, but results in some higher outliers**

Agreement between AMIENext estimations and DMSP observations are comparable to that between Iridium and DMSP observations.

Future work

- We will look into the influence of constructing the background model error covariance in different ways in terms of the time-dependent coefficients $\alpha^{(i)}$.
- Optimal settings will be determined for various time scales and characteristics of different solar wind drivers. We will study more events in particular three categories of solar wind drivers (Richardson and Cane, 2012)
  - corotating high-speed stream
  - slow flow
  - transient flows originating with CMEs.

References And Acknowledgements

We thank the AMPERE team and the AMPERE Science Center for providing the Iridium-derived data products.

Cousins, E. D. P., Matsuo, T., Richmond, A. D., & Anderson, B. J. (2015). Dominant modes of variability in large-scale Birkeland currents. *Journal of Geophysical Research: Space Physics*, *120*(8), 6722-6735.

Knipp, D. J., Matsuo, T., Kilcommons, L., Richmond, A., Anderson, B., Korth, H., ... & Parrish, N. (2014). Comparison of magnetic perturbation data from LEO satellite constellations: Statistics of DMSP and AMPERE. *Space Weather*, *12*(1), 2-23.

Matsuo, T., Knipp, D. J., Richmond, A. D., Kilcommons, L., & Anderson, B. J. (2015). Inverse procedure for high-latitude ionospheric electrodynamics: Analysis of satellite-borne magnetometer data. *Journal of Geophysical Research: Space Physics*, *120*(6), 5241-5251.

Matsuo, T., Richmond, A. D., & Nychka, D. W. (2002). Modes of high-latitude electric field variability derived from DE-2 measurements: Empirical Orthogonal Function (EOF) analysis. *Geophysical research letters*, *29*(7).

Richardson, I. G., & Cane, H. V. (2012). Solar wind drivers of geomagnetic storms during more than four solar cycles. *Journal of Space Weather and Space Climate*, *2*, A01.

Richmond, A. D., & Kamide, Y. (1988). Mapping electrodynamic features of the high-latitude ionosphere from localized observations: Technique. *Journal of Geophysical Research: Space Physics*, *93*(A6), 5741-5759.

Weimer, D. R. (2005). Improved ionospheric electrodynamic models and application to calculating Joule heating rates. *Journal of Geophysical Research: Space Physics*, *110*(A5).